dWatch: A Reliable and Low-Power Drowsiness Detection System for Drivers Based on Mobile Devices

TIANZHANG XING, School of Information Science and Technology, Shaanxi International Joint Research Centre for the Battery-Free Internet of Things, Northwest University
QING WANG, School of Information Science and Technology, Northwest University
CHASE Q. WU, Department of Computer Science, New Jersey Institute of Technology
WEI XI, Department of Computer Science and Technology, Xi'an Jiaotong University
XIAOJIANG CHEN, School of Information Science and Technology, Shaanxi International Joint Research Centre for the Battery-Free Internet of Things, Northwest University

Drowsiness detection is critical to driver safety, considering thousands of deaths caused by drowsy driving annually. Professional equipment is capable of providing high detection accuracy, but the high cost limits their applications in practice. The use of mobile devices such as smart watches and smart phones holds the promise of providing a more convenient, practical, non-invasive method for drowsiness detection. In this article, we propose a real-time driver drowsiness detection system based on mobile devices, referred to as dWatch, which combines physiological measurements with motion states of a driver to achieve high detection accuracy and low power consumption. Specifically, based on heart rate measurements, we design different methods for calculating heart rate variability (HRV) and sensing yawn actions, respectively, which are combined with steering wheel motion features extracted from motion sensors for drowsiness detection. We also design a driving posture detection algorithm to control the operation of the heart rate sensor to reduce system power consumption. Extensive experimental results show that the proposed system achieves a detection accuracy up to 97.1% and reduces energy consumption by 33%.

CCS Concepts: • **Human-centered computing → Ubiquitous and mobile computing**; **Ubiquitous and mobile devices**;

Additional Key Words and Phrases: Mobile computing, sensors, drowsiness detection, heart rate variability, smart watches

This work was supported in part by China NSFC Grant (No. 61672428, No. 61672427 and No. 61772413), the China Postdoctoral Science Foundation (No. 2017M613187), the International Cooperation Project of Shaanxi Province (No. 2020KW-004), and the Shaanxi Science and Technology Innovation Team Support Project under grant agreement (No. 2018TD-026).
Authors' addresses: T. Xing and X. Chen (corresponding author), School of Information Science and Technology, Shaanxi International Joint Research Centre for the Battery-Free Internet of Things, Northwest University, North Taibai Avenue, Xi'an, China; emails: {xtz, xjchen}@nwu.edu.cn; Q. Wang, School of Information Science and Technology, Northwest University, North Taibai Avenue, Xi'an, China; email: qwang@stumail.nwu.edu.cn; C. Q. Wu, Department of Computer Science, New Jersey Institute of Technology, Newark, NJ, USA; email: chase.wu@njit.edu; W. Xi, Department of Computer Science and Technology, Xi'an Jiaotong University, Xianning West Road, Xi'an, China; email: weixi.cs@gmail.com.

1550-4859/2020/09-ART37 $15.00
https://doi.org/10.1145/3407899

ACM Reference format:
Tianzhang Xing, Qing Wang, Chase Q. Wu, Wei Xi, and Xiaojiang Chen. 2020. dWatch: A Reliable and Low-Power Drowsiness Detection System for Drivers Based on Mobile Devices. *ACM Trans. Sen. Netw.* 16, 4, Article 37 (September 2020), 22 pages.
https://doi.org/10.1145/3407899

1 INTRODUCTION

Traffic accidents caused by drowsy driving result in severe casualties and property losses. According to the National Highway Traffic Safety Administration, drowsy driving causes more than 100,000 car crashes and 1,550 deaths each year, and 20–30% of road deaths are directly related to driver drowsiness [29]. Therefore, drowsiness detection is a major concern in relevant business sectors and research communities. For example, it has become a common policy in many insurance companies to collect the driving data of a customer for driving habit evaluation, which is then used in decision making for insurance renewal. In academia, a variety of systems have been proposed for drowsiness detection.

Among the existing methods for drowsiness detection, those based on physiological signals are considered to be the most accurate, and the Electroencephalograph (EEG) signal is often used as the standard for drowsiness detection, followed by the Electrocardiograph (ECG) signal [6, 30]. However, such methods typically require the attachment of multiple electrodes or patches to the human body, which is invasive and affects the driver's operation. Also, such methods require special equipment for medical diagnosis or research. Other computer-vision-based methods use image-processing techniques to explore driver behavior characteristics (such as facial expressions, yawn actions, blink intervals, etc.) to determine the driver's fatigue state. Although digital cameras are embedded in most mobile devices, the accuracy of these methods largely depend on the ambient light and angle of the CCD (Charge Coupled Device) [25, 27]. Another type of methods explore the motion characteristics of the vehicle (such as steering wheel movement, speed variability, lateral position, etc.), but the accuracy is limited compared with other methods [19].

A driving drowsiness detection device needs to meet four requirements, i.e., non-intrusiveness, low cost, high precision, and low power consumption. We summarize in Table 1 the performance of the aforementioned three types of methods in terms of accuracy, power consumption, interference, and cost. Most of these methods suffer from several shortcomings, such as the use of dedicated equipment and low accuracy, which limit their applications in practice. Thus, the goal of our research is to develop an accurate, non-intrusive, and low-power monitoring system without any special equipment to detect drowsy driving. Since most wearable devices (smartwatches, wristbands, etc.) are now equipped with multiple sensors and are ubiquitously used, our system is developed based on such devices to facilitate its wide use in real-life environments.

In this article, we propose a drowsiness detection system for drivers primarily based on sensor data collected by a smartwatch, which is non-intrusive and of low cost. However, we still need to meet two other requirements, i.e., high accuracy and low power consumption. Our key idea is to use the heart rate sensor combined with the data collected by motion sensors such as accelerometers and gyroscopes to extract multi-dimensional features (i.e., physiological parameter features, driver behavior features, and vehicle behavior features) that reflect the driver's fatigue state. Based on such sensor data from the smartwatch, we calculate the driver's heart rate variability (HRV), which is a key indicator for drowsiness [1], in combination with yawn actions and vehicle steering motions to detect driving drowsiness. Moreover, to reduce the power consumption of the system, we design a driver driving posture detection algorithm to control the operation of the heart rate sensor, which is typically of high power consumption, only during the driving state.

Table 1. The Summary of Existing Methods

Method	Accuracy	Power consumption	Interference	Cost
Physiological signals (e.g., EEG, ECG, etc.)	High	High	Yes	High
Computer vision techniques (e.g., yawning, blink, etc.)	High	High	No	Moderate
Motion sensors (e.g., accelerometer, gyro, etc.)	Low	Low	No	Low

There are three key technical challenges in the system design and implementation. The first challenge is to calculate the heart rate variability (HRV) based on the heart rate data collected by common sensors embedded in a smartwatch. Note that HRV is the RR interval (RRI) fluctuation of an ECG typically measured by professional medical equipment. VitaMon [15] uses a deep neural network to extract spatial and temporal information from captured facial videos to reconstruct the pulse waveform signals used to estimate RRI, and its measurement results will be affected by light intensity. In our work, the heart rate data from the smartwatch is insufficient to obtain the interval between two adjacent heartbeats as in ECG signals. To address this challenge, we conduct statistical processing of heart rate (SP-HR) to calculate the RR interval between two adjacent heartbeats, and then calculate HRV features based on these RR intervals.

The second challenge is to detect yawn actions that frequently occur in drowsiness, by exploiting only the heart rate sensor, since most existing smartwatches are not equipped with a camera. Medical study shows that yawning would cause the heart rate to rise instantaneously and drop rapidly to the normal level. This unique pattern may be used to improve detection accuracy. To address this challenge, we propose a model to match heart rate sequence and yawning (HYM) to detect the pattern's profile (e.g., the resting, ascending, and descending segments of the heart rate sequence) and further calculate the probability of yawning.

The third challenge is to design a device operation control algorithm to reduce the power consumption of the heart rate sensor. As in WSNs [2, 24], a continuous operation of the heart rate sensor may quickly deplete the energy. As the most common way to measure heart rate in smartwatches, the reflective optoelectronic method measures heart rate by measuring the blood flow at the bottom of the LED, which is a very power-consuming process with a power higher than inertial sensors (accelerometer, gyroscope, etc.) in smartwatches. To address this challenge, we design a driving posture detection algorithm by using inertial sensors to start operating the heart rate sensor only when a unique driving posture of the driver is detected.

The contributions of our work are summarized as follows:

1) We propose a novel drowsiness detection system that exploits the characteristics and actions of drowsiness driving.
2) We design different methods for calculating HRV and sensing yawn actions, respectively, by only utilizing heart rate data.
3) We design a driving posture detection algorithm as a control mechanism to start the operation of the heart rate sensor only as needed to reduce the power consumption of the system.
4) We implement dWatch and evaluate its detection performance in various scenarios, and the experimental results illustrate the efficacy of the system.

The rest of this article is organized as follows: We present some preliminaries in Section 2. We describe the architecture of dWatch in Section 3. We elaborate the design of dWatch in Section 4

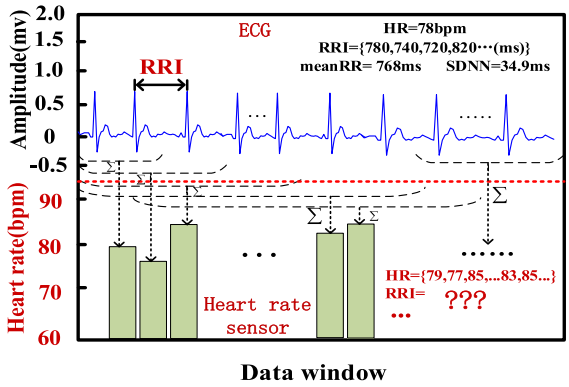

Fig. 1. Comparison of ECG and heart rate sensor.

and evaluate its performance in Section 5. We describe the related work in Section 6. Section 7 concludes our work.

2 PRELIMINARIES

2.1 Heart Rate Variability

Drowsiness is characterized by an increase in parasympathetic nerve activity or a decrease in sympathetic nerve activity, and there is a significant change in autonomic nervous system (ANS), which is an essential characteristic of the human body [4, 12]. ANS activity changes during stress, extreme fatigue, and sleepiness episodes [10]. Heart rate and rhythm are largely regulated by ANS, which can be estimated from HRV signals obtained from ECG. Therefore, drowsiness, an instinctive emotional state of the human body, can be sensed by analyzing HRV.

HRV signal is defined as the constant change of the interval between heart rates [21]. There are several HRV features commonly used for drowsiness detection.

RR Interval (RRI). A typical electrocardiographic trajectory of the cardiac cycle (standard lead II) consists of several peaks, the highest of which is called the R wave. The RRI [ms] is the interval between the R wave and the next R wave.

The following time-domain features are calculated directly from the raw RRI data.

- meanNN: Mean of RRI.
- SDNN: Standard deviation of RRI.
- rMSSD: Root mean square of difference of adjacent RRI, which reflects a rapid change of HRV.

The main frequency-domain features are as follows:

- LF: Power in the low frequency range (0.04 Hz–0.15 Hz) of PSD, which reflects sympathetic nervous system activity and parasympathetic nervous system activity.
- HF: Power in the high frequency range (0.15 Hz–0.4 Hz) of PSD, which reflects the activity of parasympathetic nervous system.
- LF/HF: Ratio of LF to HF, which represents the balance between sympathetic and parasympathetic nervous system activities.

As shown in Figure 1, the RRI can be obtained directly from the ECG, and the time- and frequency-domain features can be calculated from the RRI. We need to analyze and extract each

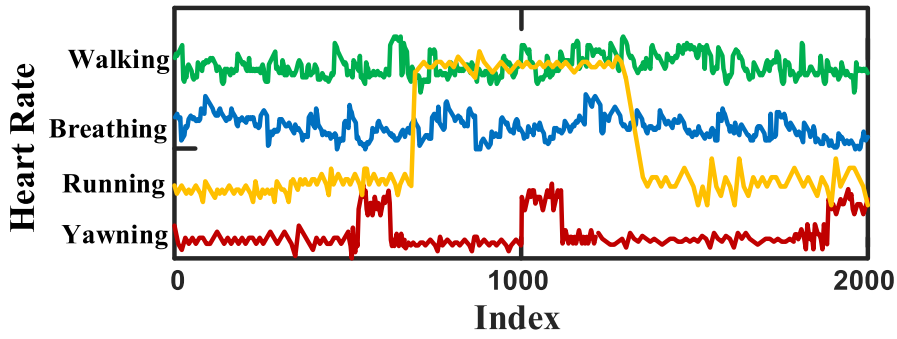

Fig. 2. A unique pattern in heart rate change during yawning.

parameter from the heart rate data of a smartwatch, and the first challenge we face is how to get the RRI from the heart rate data.

2.2 Yawning Pattern

When people feel drowsy, there are usually some accompanying physiological reactions, such as sore eyes, heavy head swell, yawning, and so on. A previous study has shown that yawning is an important indicator of human drowsiness [14].

Traditional yawning detection is to locate the person's mouth through image processing: if the mouth is detected to be open, it concludes a yawning action [17]. However, this method may lead to a false detection because the person needs to open the mouth when speaking or singing. In addition, some people usually cover their mouths with hands when yawning. In this case, the method for drowsiness detection based on mouth opening does not work. Since heart rate and heart rate variability are important indicators of drowsiness, we also collect and analyze heart rate data when people yawn. We observe an interesting phenomenon: when people yawn, the heart rate data shows a rising interval. Especially, a significant increase in the heart rate is observed at the peak of yawning compared to the baseline and it may last for at least 6 seconds. We found that this phenomenon is ubiquitous and is consistent with the study of Corey et al. [8].

However, there are many factors that could cause the heart rate to rise, such as running, listening to music, and nervousness. Therefore, to verify if the heart rate change pattern caused by yawning is unique, we collect the heart rate data at the time of different activities, as shown in Figure 2. During running, the heart rate increases from normal to maximum and remains for a period of time. After the event, the heart rate slowly returns to normal. There is no obvious change in the heart rate during walking and breathing, and it is in a relatively stable range of variation. However, the impact of yawning on heart rate presents a regularity and is different from other activities. Hence, we can detect if the driver is yawning by detecting changes in the heart rate, and we use yawn as one of the classification features to improve the detection accuracy of the system.

2.3 Built-In Sensors

The heart rate sensor detects heart rate by PPG (Photoplethysmography). The principle is that the LED behind the watch emits green light, and the photodiode determines the instantaneous blood flow by detecting the absorption of green light. When the heart contracts, the blood flow velocity increases, so the amount of green light absorption is large; on the contrary, when the heart is dilated, the blood flow velocity decreases, so the amount of green light absorption is small. The smartwatch can measure the heartbeat by detecting hundreds of green light exposures per second and changes in the regularity of green light absorption.

The accelerometer is an inertial sensor, which is triaxial accelerometer used to detect the acceleration on the x, y, and z axes of the equipment, always embedded in the smartphone and smartwatch. The essence of the accelerometer is to measure the deformation of the sensitive components inside the sensor caused by the force, and transform the deformation into an electrical signal output with the relevant circuit to obtain the corresponding acceleration signal. The three-axis acceleration sensor can fully and accurately reflect the motion properties of the object.

The three-axis gyroscope is also one of the most commonly used inertial sensors in mobile devices, which can detect the angle of rotation of the device. Its output is instantaneous angular velocity, which is need to be integrated to obtain the amount of angular variation of the device. The target angle is the initial angle plus the amount of change. The orientation of a moving object can be accurately determined by the gyroscope.

Using one single feature for driver fatigue detection may suffer from poor environmental adaptability. For example, under some road conditions, the steering wheel movement is not completely dependent on the driver's operation, and could change due to the vibration of the vehicle itself. Hence, using steering wheel movements as a sole indicator of fatigue driving behavior may lead to unreliable detection. On the other hand, the heart rate reflects changes in one's fatigue status, and is generally not affected by road conditions. However, since commercial smart devices are not as accurate as professional medical equipment for heart rate measurement, therefore, there are certain reliability problems when using the heart rate variation alone to detect driver fatigue. Note that in today's smartwatches, heart rate sensors, accelerometers, and gyroscopes provide us a convenient way to monitor the driver's physiological and sports signals. Therefore, in this work, we extract the driver's fatigue physiological characteristics and the steering wheel motion characteristics from the heart rate data and the sports data, respectively, and combine both measures to detect the driver's driving fatigue.

3 AN OVERVIEW OF DWATCH

dWatch is a drowsy driving detection system, which combines the driver's physiological parameters, behavioral characteristics, and vehicle behavior features, specifically heart rate variability features, yawning times, and steering wheel movement (turning angle, adjustment times). Since yawn detection is based on the distribution of heart rate data, it is classified as physiological representation together with heart rate variability features. The steering wheel motion feature is extracted by detecting the motion of the driver's hand, so it is classified as the driver's motion state along with the driving posture to assist in the detection system and reduce power consumption. The architecture of dWatch is comprised of three main modules, as shown in Figure 3.

In the motion state module, the system uses the data collected by the inertial measurement unit in the smart watch and smartphone to detect the driver's driving posture and steering wheel movement. Low-power listening algorithm exploits the driver's driving posture in the vehicle environment as the start-up mechanism for heart rate collection. If the driver's driving posture is detected, the heart rate sensor is activated to collect heart rate data; otherwise, it would continue to operate with low-power listening in a cycle. After the heart rate sensor is activated, the system extracts drowsiness-related features such as the number of adjustments on the steering wheel and the turning angle from the movement data of the steering wheel.

In the physiological representation module, the heart rate data is processed in two aspects: (i) heart rate data is transformed into HRV through the proposed SP-HR method, (ii) the proposed HYM detects the yawning action as an indicator of drowsiness. Specifically, the probability of yawning is calculated by the transition probability of heart rate sequence (TPH), heart rate segment detection (HSD), PuH estimation.

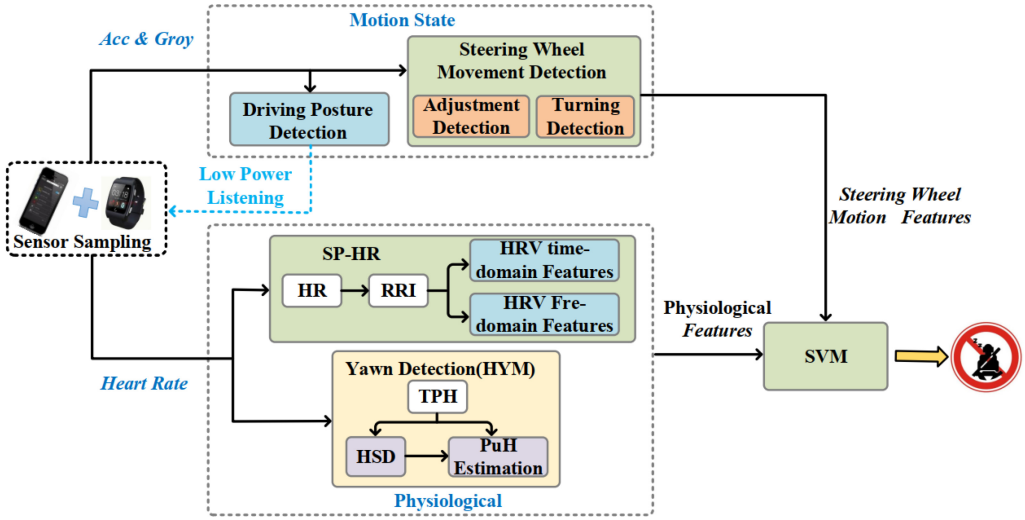

Fig. 3. System Architecture of dWatch.

In the classification module, we employ SVM as a classifier, which uses a Gaussian radial basis function as a kernel function to map data to the feature space. Features extracted from the above module are the input data for the classifier. The classifier quickly processes the newly entered samples and outputs the driver's current state. Finally, according to the classified result, dWatch takes a corresponding action.

In our system, the heart rate sensor and inertial sensor signals are subject to some noise interference during monitoring. Normally, the heart rate data is relatively stable, and even in the case of sudden tension, it does not vary significantly during a short period of time. Hence, we fit a linear function in the heart rate data over a small time window $t = 6s$ to clean out the abnormal heart rate data that deviates from the linear function beyond the threshold. Also, vehicle motion may cause interference to steering wheel motion. To account for such noise, we use the inertial sensor in a smartphone to detect the movement of the vehicle, and remove this component from steering wheel motion as part of the data preprocessing, as detailed in Section 4.3.2.

4 SYSTEM DESIGN

In this section, we describe the design details of the system. It mainly includes HRV feature extraction method (named SP-HR), yawn detection, steering wheel motion feature extraction and driving posture detection algorithm designed to reduce power consumption.

4.1 Statistical Processing of Heart Rate (SP-HR)

The heart rate variability (HRV) feature commonly used for fatigue detection is the result of time-domain statistics and frequency-domain transformation of adjacent heartbeat intervals (RRI). Traditional HRV is measured by electrocardiograph or PPG, which uses a contact signal measurement method and is inconvenient in driving environments. Recent work uses a smart phone's camera to capture subtle changes in the face or finger skin to reconstruct the pulse signal [15]. Note that this method may undermine user privacy, and nevertheless, most existing smartwatches are not equipped with cameras. The heart rate sensor of a smart watch provides a more convenient method for signal detection. However, due to its closed API, the smart watch cannot directly measure HRV or provide fine-grained RRI, but only heart rate data. Therefore, one must extract HRV features

from the heart rate, and according to the definition of HRV, RRI needs to be calculated first. In this work, we propose an HRV feature extraction method based on statistical analysis, calculate RRI from heart rate data, and then perform time-frequency domain analysis to obtain the time-frequency domain features of HRV, as detailed.

We collect a large amount of heart rate data from different users in different scenarios. According to the HRV analysis guidelines, RRI should be measured for at least 2 to 5 minutes for accurate frequency analysing. We design a sliding window w_h to extract the heart rate sequence, and w_h = 300 represents 300 consecutive heart rate data items over a time duration of about 5 minutes.

Assume that the heart rate data sequence is $H_n = \{h_n, h_{n-1}, h_{n-2}, \ldots, h_{n-(w_h-1)}\}$, the average value of the w_h data items is denoted as R, i.e., $R = (h_n + h_{n-1} + h_{n-2} + \cdots + h_{n-(w_h-1)})/w_h$. The total number of heartbeats in 5 minutes is $5R$, and the number of RRI is $5R - 1$. We first calculate the inverse of w_h data items separately, and then multiply each by 60 to obtain $H'_n = \{60/h_n, 60/h_{n-1}, 60/h_{n-2}, \ldots, 60/h_{n-(w_h-1)}\}$, which represents w_h RR intervals. The remaining $5R - 1 - w_h$ RR intervals are generated by two methods: one is to calculate the mean value of w_h RR intervals, and the other is to calculate the maximum and minimum values of w_h RR intervals, and then use the random number generator to generate random numbers in the range between the minimum and maximum values. In this work, we use random numbers to generate the remaining RRI, which is more in line with the user's heartbeat changes.

RRI data is not directly used for clinical testing, and further extraction of HRV time- and frequency-domain features is required. As mentioned above, the time-domain features include meanNN, SDNN, and rMSSD, calculated as follows:

$$\text{meanNN} = \left(\sum_{i=1}^{N} RRI_i\right) \Big/ N, \tag{1}$$

$$SDNN = \sqrt{\frac{1}{N}\sum_{i=1}^{N}(RRI_i - meanNN)^2}, \tag{2}$$

$$rMSSD = \sqrt{\frac{1}{N-1}\sum_{i=1}^{N}(RRI_{i+1} - RRI_i)^2}. \tag{3}$$

Where N is the number of heart rate data, in our work $N = w_h = 300$.

The time domain analysis method of HRV analysis has the advantages of simple calculation and intuitive index meaning. However, this method cannot describe the dynamic process of HRV, and it is difficult to further distinguish the level of sympathetic nerve and vagus nerve activity. The frequency domain analysis method can describe the energy distribution of heart rate fluctuation signals according to different frequency bands. It is sensitive and accurate, which makes up for the shortcomings of time domain analysis.

The spectrum analysis of HRV mainly includes the classic spectrum estimation method and the modern spectrum estimation method to perform spectral estimation on the RR interval series. The parametric model spectral estimation method commonly used in modern spectral estimation methods has the advantages of smooth spectral lines and high resolution. However, the modeling process is complicated, the model order is difficult to determine, and the data is required to be a stationary sequence. In contrast, HRV classic spectral estimation method has simple algorithm (implemented by fast Fourier transform), fast operation speed, and can well reflect the trough.

In this article, we use the autocorrelation method in classical spectral estimation methods. Specifically, according to Wiener, Sinchin's theorem is as follows: First, estimate the autocorrelation function $R_x(m)$ of the sampled data $x(n)$, then find the Fourier transform of $R_x(m)$, and

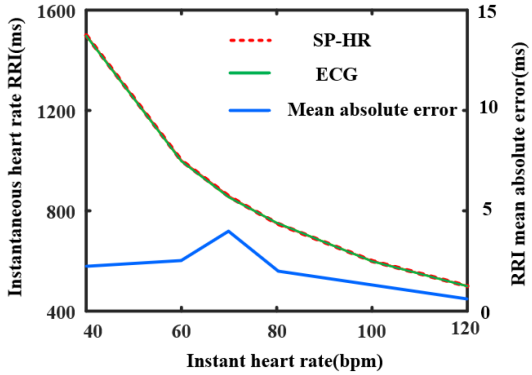

Fig. 4. RRI mean absolute error of different instantaneous heart rates.

then get the power spectrum of $x(n)$:

$$\hat{P}_{bt}(f) = T \sum_{k^{m-n}}^{M} w(k) R_x(k) e^{-j2\pi f k T} \tag{4}$$

where $w(k)$ is the lag window, $M \leq N - 1$. Commonly used frequency-domain features include LF, HF, and LF/HF. In clinical application, 0.15 Hz is often used as the dividing line between low-frequency components (≤0.15 Hz, LF) and high-frequency components (>0.15 Hz, HF). The LF component mainly represents the sympathetic nerve or the dual effects of the sympathetic nerve and the vagus nerve. The HF component only reflects the vagus nerve activity. The ratio of the LF component to the HF component energy (LF/HF) can be used to reflect the sympathetic and vagal nerve activity balance.

In the experiment, we tested the performance of the SP-HR method. We collected the ECG data of 28 volunteers with driving experience on the driving simulator, and also collected the heart rate data of 22 ordinary people under non-driving simulation conditions. Figure 4 shows the average absolute error of RRI corresponding to different instantaneous heart rates when the RRI calculated from the heart rate data using this algorithm is compared with the RRI on the electrocardiogram. We observe that the maximum RRI mean absolute error is less than 4 ms, and the average value of all the RRI mean absolute error is about 1.5 ms, which is a relatively low. These results show that our heart rate data processing method has good performance for RR interval extraction, and lays down a solid foundation for HRV time-frequency domain analysis. The results of HRV time-frequency domain feature extraction are provided in Section 5.2.

4.2 Heart Rate Sequence Yawn Matching Model (HYM)

We propose HYM, which on the basis of universality of on the change of heart rate caused by yawning. The problem of yawning can be described as: (1) Heart rate sequence corresponding to the event; (2) The probability of transition for heart rate; (3) The probability of yawning.

4.2.1 The Transition Probability of Heart Rate Sequence (TPH). In this model, we first fit the sampled discrete heart rate data using the least squares method. Then, we get a series of heart rate sequences $H_n, H_{n-1}, H_{n-2}, \ldots, H_{n-w}$ from the smooth heart rate analyzing at w. Specifically, assuming that the currently detected heart rate is h_n, the heart rate sequence is:

$$H_n = \{h_n, h_{n-1}, h_{n-2}, \ldots, h_{n-(w-1)}\} \tag{5}$$

where w is a sliding window for heart rate analysis, n is a positive integer. Usually yawning time is 6 to 10 seconds or so with no obvious periodicity. In order to be consistent with the analysis of HRV, we set $w = w_h = 300$.

The $P(h_i/H_{(i-1)})$ is defined as transition probability between any heart rate. Thus, the probability of a specific event which, following the heart rate sequence $\{h_{n-1}, h_{n-2}, \ldots, h_{n-w}\}$, is estimated as:

$$P_{event} = \prod_{i=n-w}^{n-1} \mathrm{P}(h_i/H_{i-1}). \tag{6}$$

P_{event} may be the probability of yawning or non-yawning. The probability that the user performs non-yawning can be quantified by P_{event} (denoted as P_oY). We have:

$$P_oY = \min\left\{\frac{P_{event} - \min(P_s)}{\max(P_s) - \min(P_s)}, 1 - P_{event}\right\}, s \in S, \tag{7}$$

where S is the set of all possible heart rate sequences. P_s presents the probability of performing an event follows the sequence s. Following the heart rate sequence H_n, the probability of yawning is denoted as $P_{yawn}(H_n)$:

$$P_{yawn}(H_n) = P_oY \cdot P_uH, \tag{8}$$

where P_uH indicates the probability of yawning; specifically, we use the Euclidean distance matching algorithm (ED) to calculate the P_uH.

4.2.2 Heart Rate Segment Detection (HSD). In order to accurately estimate the P_uH, the heart rate should be segmented. In this process, we design the sliding window. It is used to segment the heart rate data and extract the ascending, descending, and resting state sequences.

(i) *Resting Heart Rate Detection.* Under normal circumstances, this is the heart rate at a state of equilibrium. There are multiple consecutive sliding windows, and the average value of each sliding windows is fluctuating in the same horizontal range. Initial average resting heart rate h_r can be obtained.

(ii) *Heart Rate Rise Detection.* Similarly, when the average value of each sliding window is increased, we determine that the heart rate is in the rising phase, the time at the 1th sliding window is the ith initial rise time, which is recorded as t_{ui}.

(iii) *Heart Rate Drop Detection.* When the average value of each sliding window decreases, we determine that the heart is in the falling phase, the time of the 1th sliding window is the first initial falling time, expressed as t_{di}.

And then, return to the resting heart rate detection, the time at the second sliding window is the (i+1)-th initial rest time, denoted as $t_{r_{i+1}}$. Therefore, the time T_i of the ith yawning effect on heart rate is:

$$\mathrm{T}_i = t_{r_{i+1}} - t_{ui}. \tag{9}$$

The amount of time each person yawns varies little. Thus, we propose a limit factor Q to indicate the similarity between the T_i and T_{i+1}.

$$Q \approx \frac{P\left(T_{i+2}/T_{i+1}\right)}{P\left(T_{i+1}/T_i\right)}. \tag{10}$$

The greater the value of the parameter Q, the greater the probability of user yawning. Otherwise, the probability is smaller.

4.2.3 P_uH Estimation. In order to obtain accurate $P_{yawn}(H_n)$, we design a separate P_uH estimation method by calculating the similarity of the ascending and descending segments of the heart rate. When the PuH is at heart rate rising phase, ED method was used to quantify the similarity of ascending segment of window. When yawning, the heart rate sequence can be divided into ascending segment, descending segment, and resting segment. Assuming H_{U_i} is the ascending segment, then $H_{U_{i+1}}$ is descending segment, $H_{U_{i+2}}$ is rest segment, and $H_{U_{i+3}}$ is the next ascending segment. The Euclidean distance of the rising segment is:

$$\mathrm{E}_r(H_{U_i}, H_{U_{i+3}}) = \frac{\min((H_{U_1} - H_{U_4}), \ldots, (H_{U_i} - H_{U_{i+3}}))}{T}, \tag{11}$$

where T is the time of the heart rate sequence when yawning.

Similarly, the Euclidean distance of the descending segment is:

$$\mathrm{E}_d(H_{U_{i+1}}, H_{U_{i+4}}) = \frac{\min((H_{U_2} - H_{U_6}), \ldots, (H_{U_{i+1}} - H_{U_{i+4}}))}{T} \tag{12}$$

The smaller $E_r\ (H_{U_i}, H_{U_{i+3}})$ and $E_d\ (H_{U_{i+1}}, H_{U_{i+4}})$ are, the probability of yawning is higher. The P_uH can be calculated as

$$P_uH = (1 - E_r\ (H_{U_i}, H_{U_{i+3}}) \cdot E_d\ (H_{U_{i+1}}, H_{U_{i+4}})) \cdot Q \tag{13}$$

According to the experimental results, we set the detection threshold to 0.4. The event sequence is considered to be yawning when the $P_{yawn}(H_n) \geq 0.4$.

4.3 Motion Sensors Module

Due to the high power consumption of the heart rate sensor, we have designed a driving posture detection algorithm to reduce the power consumption of the dWatch that is based on the user's hand motion. The main idea is to wake up the heart rate sensor so that it works when the unique driving posture of the driver [5] is detected; otherwise, it is asleep. In addition, in order to improve the detection accuracy of the dWatch, we also considered method based on the vehicle behavior characteristics (e.g., steering wheel movement, vehicle driving direction, vehicle speed), which is also an objective driver-drowsiness-detection method [13, 23]. Since we use inertial sensors in smartwatches to track the driver's hand movements, in this work, we only considered one of the vehicle behavior characteristics, the steering wheel motion features. Specifically, we extract steering wheel motion features from inertial sensor data in smartwatches and smartphones as auxiliary features of physiological features to improve the detection accuracy of the system.

4.3.1 Driving Posture Detection Algorithm. In order to reduce the power consumption of the system, we designed a driving posture detection algorithm when the driver holds the steering wheel. Because before driving or while driving, the driver needs to hold the steering wheel to control the direction of the vehicle , and the arm will stretch forward and the elbow will lie naturally when the driver holds the steering wheel (as shown in Figure 5(a)), a unique pattern is created when detecting the posture of the smartwatch worn on the driver's wrist.

The component of measurements from the accelerometer is shown in Figure 5(b), where g represents the virtual acceleration generated by gravity G interference, a is the sum of g and the true acceleration a_L, and a_L can be decomposed into horizontal acceleration a_h and vertical acceleration a_v. Since the direction of the x-axis on the smartwatch is always parallel to the forearm, the average value of g on the x-axis in a window, which is denoted as $g_{x,watch}$, is used to characterize the driving posture because different hand postures produce different acceleration measurements. For example, when the driver holds the steering wheel, $g_{x,watch}$ is about $-3.46\,\mathrm{m/s^2}$; when the driver drinks water, the forearm is raised, and $g_{x,watch}$ is about $-8.32\,\mathrm{m/s^2}$.

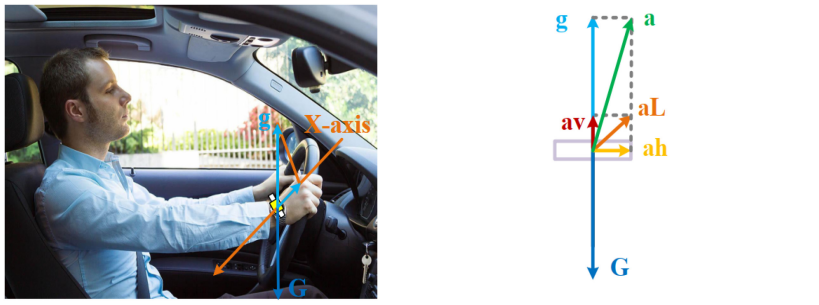

(a) A typical driving posture

(b)The component of measurement from accelerometer

Fig. 5. A typical driving posture.

Because the driver's driving posture when holding the steering wheel is similar to the posture of other events, such as the user holding a book on the table with both hands or holding the left and right sides of an iPad, only $g_{x,watch}$ is used to detect the forearm gesture of the driver's hand holding the steering wheel is not enough. So we introduce the vibration signal in the vertical direction, which is one feature that detects whether the driver's hand is on the steering wheel in [5]. When the engine of the vehicle is started, continuous vibration in the vertical direction is generated and radiated into the cockpit. If the driver holds the steering wheel, the amplitude of the vibration transmitted to the driver's wrist through the steering wheel would be much stronger than the vibration transmitted through the seat. However, the motion of the vehicle interferes with the vibration signal, so we place a smartphone in the vehicle to monitor the motion of the vehicle. Since the vibration signal of interest is mainly in the vertical direction, we first solve the vertical component as follows:

$$\mathrm{a}_v = \overrightarrow{g} \bullet \overrightarrow{a_L}/|\overrightarrow{g}|. \tag{14}$$

The amplitude of the vibration can be obtained by calculating the a_v variance, and the interference caused by the vehicle moving in the vertical direction is estimated by measuring the a_v of the smartphone. The system mitigates interference by calculating:

$$R_{av} = \frac{VaR(\mathrm{a}_v, watch)}{VaR(\mathrm{a}_v, phone)}. \tag{15}$$

If the vibration is mainly caused by the motion of the vehicle, $VaR(\mathrm{a}_v, watch)$ is greater than 0.04, and its distribution cannot be used as an evidence for detecting the posture of the forearm. But if the driver holds the steering wheel, the vertical movement of the wrist is similar to the vehicle. Specifically, we build a vector $f = \langle g_{x,watch}, VaR(\mathrm{a}_v, watch), R_{av}\rangle$ and a training dataset that include only data samples when the hand is on the steering wheel. For test data, the classifier computes the probability of the test data fitting into the distribution of the training dataset by the statistical hypothesis testing, similar to the definition of outliers in [33]. The test samples that fit into the distribution of the trained model are classified as the defined driving posture of the driver.

4.3.2 Steering Wheel Movement. Feng et al. [11] and Li et al. [22] demonstrated that the driver's adjustment times and turning angles in the state of drowsiness are significantly different from the awake state. Therefore, in order to further improve the detection accuracy of the system, we should monitor the operation of the driver on the steering wheel, such as adjustment and turn information.

(1) *Interference from Vehicle Movement.* The accelerometer is very sensitive and can be easily interfered with by vehicle movements when monitoring steering wheel movements. Therefore, before extracting the steering wheel motion characteristics, we need to denoise the collected inertial sensor data. In this work, we place a smartphone in a car to detect the movement of the vehicle, and perform a denoising process in two steps: (i) detect whether the driver's hand is moving inside the vehicle and (ii) eliminate the interference of vehicle vibration.

In the driving environment, the detection of a relative movement between the vehicle and the driver's hand can be used to indicate that the driver's hand may be operating the steering wheel. We leverage the work from Bi et al. [5] to detect if the driver's hand is moving by comparing the acceleration of the smart watch ($|\vec{a_w}|$) and the acceleration of the smart phone ($|\vec{a_p}|$) [20]. Since the coordinates of the smart phone and the smart watch are not aligned, the components of the acceleration of the two devices in various directions cannot be directly compared. However, when there is no relative movement between the two devices, the ($|\vec{a}|$) of these devices should be similar. Therefore, we can determine if the driver's hand is moving by checking the following inequality and comparing each device's ($|\vec{a}|$):

$$\frac{\sum_{l=1}^{n} ||a_{l,w}^{\vec{}}| - |a_{l,p}^{\vec{}}||}{n} \leq \mu, \tag{16}$$

where n is the length of the window. If the inequality is satisfied, it indicates that there is a relative motion between the driver's hand and the vehicle. In the experiment, $\mu = 1.02\,\mathrm{m/s^2}$.

Once a hand movement is detected, we need to remove the interference from the vehicle vibration. Hence, before extracting the steering wheel movement characteristics, we subtract the corresponding sensor data collected by the smart phone from the sensor data extracted from the smart watch to reduce the interference.

(2) Steering wheel motion feature: The adjustment is defined by linear acceleration and radial velocity were collected by the built-in accelerometer and gyroscope of the smartwatch. The linear acceleration and radial velocity are calculated by the formula (17) into resultant magnitude:

$$resultant\ magnitude = \sqrt{x^2 + y^2 + z^2}, \tag{17}$$

where x, y, and z are the linear acceleration and radial velocity in each direction, the linear acceleration in the x direction is aL in Figure 5(b). When the magnitude of any linear acceleration exceeds 1, and the magnitude of radial velocity exceeds 0.2, it is counted as 1 adjustment.

The turning situation of the vehicle is obtained by analyzing the data collected by the gyroscope on the smartphone [7], specifcally, the rotation around the direction of the gravity indicates the angle of the vehicle's turning. Utilizing data collected from the smartwatch, the steering wheel movement is computed individually for three distinct axes: pitch, roll, and yaw, which correspond to the x-, y-, and z-axis respectively; the derivation of respective angle (agl_i) for pitch at time ith is illustrated in Equation (18):

$$agl_i = 0.98 \times (\mathrm{agl}_{i-1} + gyr_i / gyr_{hz}) + aglc_i \times 0.02, \tag{18}$$

where 0.98 and 0.02 represent two different weight coefficients; and gyr_i, gyr_{hz}, and $aglc_i$ are the gyroscope sensor reading, gyroscope sampling rate, and the angular acceleration at the ith time point, respectively. The angular acceleration is calculated as follows:

$$aglc_i = \arctan(a_u, a_v) \times 180/\pi, \tag{19}$$

where a_u and a_v are the linear accelerometer readings on the y- and z-axis, multiplied by $180/\pi$ to convert the result to radians. The angle calculation is repeated similar to Equations (18) and (19), but applying the x- and z-axis for roll, the x- and y-axis for yaw angles, respectively. The

Table 2. The Classification of Drowsiness Level in dWatch

No.	Karolinska Sleeping Scale	Level of dWatch
1	Extremely alert	level 1
2	Very alert	level 1
3	Alert	level 2
4	Rather Alert	level 2
5	Neither alert nor sleepy	level 3
6	Some signs of sleepiness	level 3
7	Sleepy, but no difficulty remaining awake	level 4
8	Sleepy, some effort to keep alert	level 4
9	Extremely sleepy, fighting sleep	level 5

calculated angles represent the angles variation relative to time, and they have a correlation with the steering angle control.

Feng et al. [11] have shown that drivers have fewer steering wheel adjustments when they are awake than when they are drowsy. The average number of adjustments during waking is 26 per minute, while the average number of adjustments during slumber is only 9 per minute [22]. For the steering angle, θ is focused at $|\theta| \leq 90^{\circ}$ since the drowsiness-induced SWM factor is bounded at no more than 10^{o} angle according to current research [20]. Thus, driver drowsiness detection can be done by monitoring the number of steering wheel adjustments by hand and the steering angle.

The motion sensor module can improve the reliability of the system. By tracking the driver's hand movements, the driving behavior of the driver's steering wheel is extracted as an auxiliary feature for driver fatigue detection, which improves the environmental adaptability using a single type of signal. Also, it helps reduce the power consumption of the system and controls the working time of the heart rate sensor with high power consumption through the designed driving posture detection algorithm. Although two accelerations need to be sampled, the frequency of the accelerometer is much lower than that of the heart rate sensor, hence saving significant energy.

4.4 Classifier Training

Since our dataset consists of a small number of samples and nonlinear data, we use support vector machine (SVM) as the classifier, which has a good performance for a small sample size and on datasets with nonlinear and high-dimensional features. We use (S_i, L_i) to represent the training sample, where $S_i = \langle meanNN, SDNN, rMSSD, LF, HF, LF/HF, T_{yawn}, T_{ad}, A_{turn} \rangle$ represents the features vector representing the ith heart rate sequence, where T_{yawn} is the number of yawns, T_{ad} is the number of steering wheel adjustments, A_{turn} is turning angle of the steering wheel, and L_i represents the drowsiness level of the ith value. As shown in Table 2, L has five classes, from one to five. The idea of the classifier is to find four hyperplanes with the largest boundary that separates the five classes. In the case of linearly separable data, the hyperplane of the support vector is as follows:

$$f(S) = \sum_{i=1}^{n} a_i L_i S_i S(i) + b, \tag{20}$$

where L_i represents the class of the sample point S_i, and $S(i)$ represents the support vector machine, $a_i (i = 1, n)$ is Lagrangian multipliers. If the data is not linearly separable, first map it to

another feature space which is linearly separable by kernel function, and Equation (20) becomes:

$$f(S) = \sum_{i=1}^{n} a_i L_i \mathrm{v}(S_i, S(i)) + b. \tag{21}$$

$\mathrm{v}(\cdot)$ represents the kernel function. In dWatch, the svm classifier uses a Gaussian radial basis function to map data to another feature space. The calculation formula of Gaussian radial basis kernel function is as follows:

$$v(S_i, S_j) = exp(-\gamma \|S_i - S_j\|^2), \tag{22}$$

where γ is kernel parameter, after using the kernel function, the dual problem solved by the support vector machine during training is:

$$\begin{aligned} min_a \frac{1}{2} \sum_{i=1}^{n} \sum_{j=1}^{n} a_i a_j L_i L_j v\left(S_i^T S_j\right) - \sum_{k=1}^{n} a_k \\ s.t. \quad 0 \le a_i \le C \\ \sum_{j=1}^{n} a_j L_j = 0, \end{aligned} \tag{23}$$

where n is the number of training samples and C is the penalty factor, which is a manually set parameter. In our work, $\gamma = 5$, $C = 80$.

5 IMPLEMENTATION AND EVALUATION

Twelve healthy volunteers with at least one year of driving experience (including 9 males and 3 females, with an average age of 38 ± 15 years) were recruited to participate in our experiments. They did not have any sleep disorders, sleep apnea and other related diseases that may affect the results of the analysis. Subjects were asked to fill out survey forms before and after the experiment. In the experiment, we used the Euro track simulator, which realistically mimics different driving environments, including deceleration and parking at red lights, speed limits on highways, waiting for traffic lights at intersections, turning, and night driving. Each participant had 2 to 3 hours before the formal experiment to become familiar with the simulation system. We conducted experiments during the day and night to collect data. And in the total dataset, 70% is used for training and 30% is used for testing. During the experiment, we obtain the ground truth of the subjects through a camera, including the state of drowsiness and the operation of the steering wheel during the simulation.

We use these metrics to quantify the performance of the dWatch.

Precision: The percentage of samples accurately detected by the dWatch in the total sample.

Recall: The percentage of correctly detected samples in all relevant samples.

False Positive Rate (FPR): The percentage of non-fatigue state samples mislabeled by the algorithm as fatigue state in all non-fatigue state samples, a.k.a. false alarm rate.

False Negative Rate (FNR): The percentage of fatigue state samples mislabeled by the algorithm as non-fatigue state in all fatigue state samples.

5.1 Performance and Advantages of dWatch

The overall accuracy of the dWatch is shown in Figure 6. The accuracy is up to 97.1% and the recall is 98.3%. The performance of the system in different gender groups is similar, and the male group is closer to the total accuracy. The lower accuracy of the female group is mainly due to the smaller number of samples used for training;, however, the detection accuracy is still higher than 92.3%. The main reason is that our system extracts three types of features that characterize drowsiness.

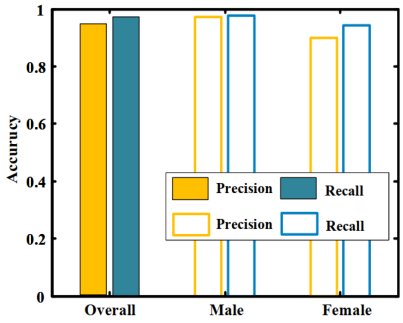

Fig. 6. Accuracy of dWatch.

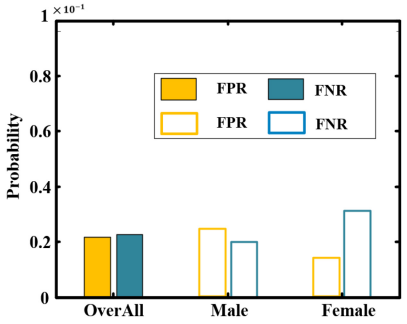

Fig. 7. False positive rate and false negative rate in different gender groups.

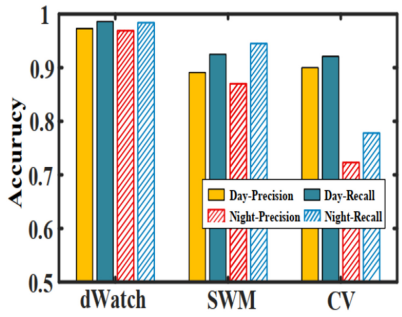

Fig. 8. Comparison with other methods.

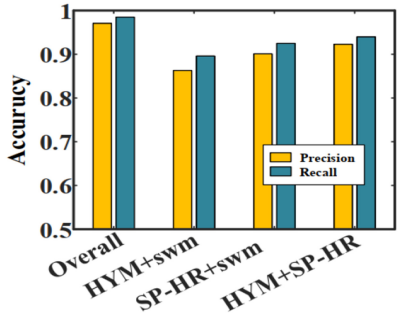

Fig. 9. The impact of each module of dWatch.

Figure 7 shows the performance measurements of the system in terms of false positive rate and false negative rate in different gender groups. We observe that the overall false positive/negative rate of the system is less than 3%. The false negative rate of the female group is higher than that of the male group, but still less than 4%. We believe that the system can operate reliably with such a low false positive/negative rate and can be a useful assisting tool to ensure safe driving.

We compare dWatch's performance during day and night through steering wheel movement (SWM) and computer vision (CV) as shown in Figure 8. We can see that the accuracy of both the SVM and CV methods has decreased at night. The CV method is especially obvious, mainly because the nighttime illumination is very different from the daytime, which seriously affects the performance of the system. The performance of the SVM method is not much different between day and night, but the overall accuracy is not high, mainly due to the small number of features detected, which cannot fully reflect the state of the driver. In comparison, dWatchis more accurate and robust, day or night. Because the HRV signals and yawning features detected by the system come from the heart rate which is hardly affected by the ambient light, and the features of the steering wheel movement are used as auxiliary features to improve the system's detection accuracy.

In order to detect the influence of various features in dWatch on system performance, we combine the features of any two of the three modules (HRV, yawn, and motion) as new samples to test the influence of the remaining features on dWatch. In Figure 9, the accuracy of the system is significantly reduced when any type of feature is missing, indicating that each type of feature has a very important effect on the system. The method of combining yawn and motion (HYM+SWM) has the lowest precision, and the method with SP-HR (SP-HR+SWM, SP-HR+HYM) has relatively

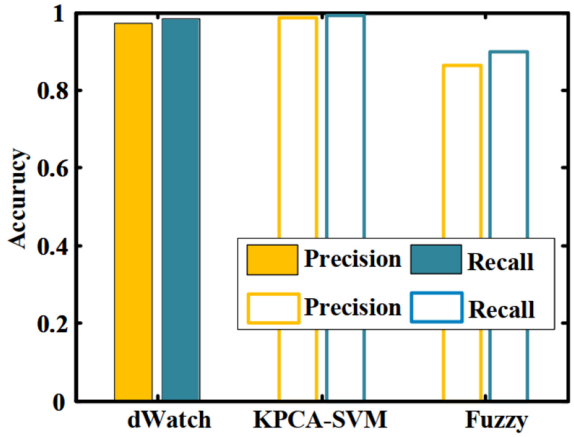

Fig. 10. Comparison with other classification.

high precision. Even when the driver's hand is away from the steering wheel and the steering wheel motion characteristics cannot be detected, the system achieves 91.5% accuracy when using only heart rate data (SP-HR + HYM) for driving fatigue detection. The main reason is that HRV can best indicate human drowsiness state among the three types of features and its weight is the largest. Therefore, when HRV is included in the feature, the classification accuracy increases and the result is more reliable.

In addtion, we compare with other classification methods. As shown in Figure 10, the accuracy of KPCA-SVM is higher than that of dWatch, but the algorithm is too complicated to be implemented on resource-constrained devices. Fuzzy is ideal for deployment in watches, but the accuracy is low. For now, considering the trade-off between complexity and precision, dWatch is better suited for deploying on smartwatches.

Although with a high level of detection accuracy, there is inevitably a missed detection event, and no accuracy standard exists in industry as a benchmark [13]. By combining driver physiological characteristics and driving behavior characteristics, our work reduces the rate of missed detection and can be used to assist in safe driving.

5.2 Comparison of SP-HR and ECG in Time-Frequency Domain Feature Extraction

To validate our proposed SP-HR, we compare the time and frequency domain features of HRV extracted from ECG and heart rate data (HR) using SP-HR method. Figure 11 and Figure 12 show that several HRV features extracted from the ECG and from HR data are approximately equal, and several other features have similar results. Since enough data is collected per unit time, the HRV features extracted after taking the average heartbeat interval as the instantaneous heartbeat interval are similar to the results from the ECG. It shows that our proposed SP-HR can be used as a method for RRI analysis of heart rate data.

5.3 Performance and Influencing Factors of HYM

HYM determines whether the driver yawns by calculating the transition probability of the heart rate sequence. When $P_{yawn}(H_n) \geq 0.4$, the heart rate sequence is considered to represent yawning. The performance of HYM is shown in Figure 13. The total detection accuracy is 91% and the recall is 94.5%. The accuracy and recall are 92.6% and 95.6% in the male group and 86.7% and 91.3% in the female group. The main reason for the low accuracy of the female group is that

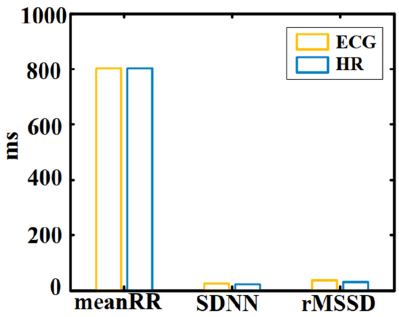

Fig. 11. HRV time domain features extracted.

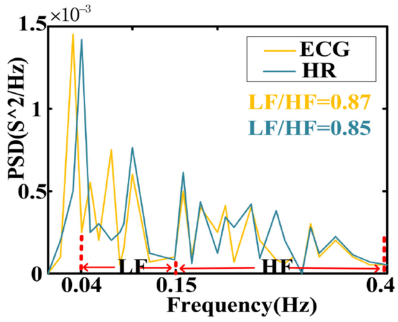

Fig. 12. HRV frequency domain features extracted.

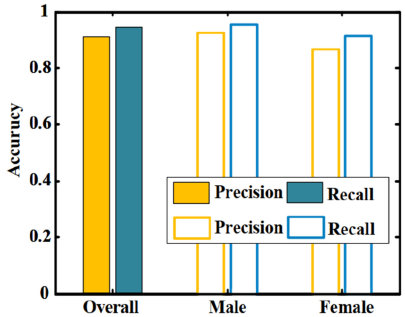

Fig. 13. The accuracy of HYM.

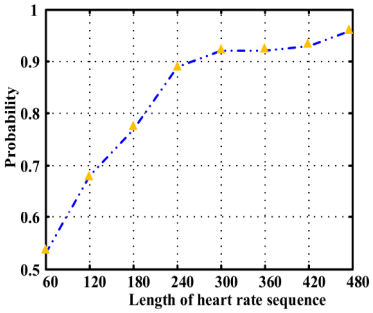

Fig. 14. The effect of the heart rate sequence.

the number of female samples collected is relatively small, there are fewer yawn events included in the sliding window. However, the detection accuracy still exceeds 85%, because our proposed HYM calculates the probability of yawning by calculating the similarity between different rising heart rate segments and falling heart rate segments.

The HYM method mainly calculates the probability of yawning by heart rate sequence segmentation and Euclidean distance matching algorithm (ED). The length of the heart rate sequence greatly affects the detection result. We have tested the yawn detection results of different lengths of heart rate sequence in the experiment. In Figure 14, it is easy to see that, as the length of the heart rate sequence increases, the accuracy of the HYM gradually increases. When the length is greater than 300, the probability of yawning is 91%. The longer the heart rate sequence, the more yawn events are included and the higher the detection accuracy.

5.4 Effect of Time on Performance of Motion Monitoring

For the driving posture detection algorithm, the model's training dataset contains only the data samples of the driver's hand on the steering wheel. For the test data, we use Welch's t-test to check whether the test sample fit into the trained model. Figure 15 presents the accuracy of driving posture detection at different length of time when the driver's hand is on the steering wheel. We can observe that as the length of time increases, the precision and the recall gradually increases, and the precision and recall are over 90% and 95%, respectively, when $t = 8(s)$. Therefore, we can achieve a good precision by letting $t = 8s$ in the experiment.

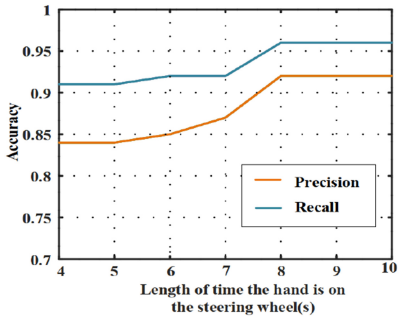

Fig. 15. The accuracy of the driving posture detection algorithm.

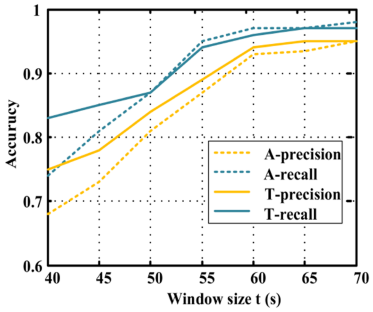

Fig. 16. The effects of data analysis window t.

In dWatch, we infer the steering wheel manipulation by tracking the movement of the driver's hand. The steering wheel manipulation is mainly divided into adjustment and turning. The performance of the steering wheel movement detection depends on the time t of the data analysis window. We tested the effects of different t on steering wheel adjustment and turning detection results. Figure 16 shows that the detection accuracy of the adjustment and turning increases with the increase of t, A means adjustment, T means turning. When the time reaches 1 minute, the accuracy exceeds 93%, and then the accuracy increases slowly. We choose t = 60s in the experiment, which is considered to be a good balance between calculation and precision.

5.5 Effect of Driving Posture Detection Algorithm on System Power Consumption

One of the biggest challenges in using a heart rate sensor on smartwatches for a full day of drowsiness detection is power consumption. In the experiment, we use a power monitor to test the power consumption of the system. When the heart rate start algorithm (driving posture detection algorithm) is not used, the smartwatch can only work for 8 hours, but it can last for 12.7 hours when using the startup algorithm, power consumption is reduced by 33% compared to before. The work time of the smartwatch is greatly extended, which is enough to monitor the driver's drowsiness throughout the day.

6 RELATED WORK

Physiological Measurement. Physiological signals are considered to be an accurate indicator of drowsiness because they are strongly related to driver fatigue [3, 10, 28, 32]. Electroencephalogram (EEG) is widely regarded as one of the most reliable physiological indicators. Previous studies have used the time and frequency characteristics of EEG signals to detect drowsiness [10]. Electrocardiogram (ECG) is another widely used method to detect sleepiness. The core of the method is to distinguish between alertness and sleepiness by extracting HRV features from ECG [21, 28, 32], although these methods provide effective detection of physiological and cognitive states of the human body. However, the feasibility of these methods in the actual driving environment is severely limited due to the wearability of the equipment; they usually need to touch the electrodes to measure the signal, which will affect the driver's comfort and interfere with driving.

Computer Vision. The computer vision method mainly uses image processing technology to detect the driver's behavior characteristics to judge the driver's drowsiness. These behavioral features mainly include head movement, blink frequency, eyelid closure, yawning, facial expressions, and the like [9, 16]. The performance of this method is greatly affected by the ambient light intensity and other factors. For example, the lighting conditions on both sides of the window vary

greatly during the day and night, and the use of glasses (affecting blink detection) and the use of the hand covering the mouth (affecting yawn detection) will reduce the performance of the image processing system. The reliability of such methods is low, although they are non-invasive.

Motion Sensors. The motion sensor method mainly detects the steering wheel movement, speed variability, lane departure of the vehicle through sensors [18], using these measurements to analyze the driver's ability to control the vehicle and judging the driver's drowsiness state. These measures are highly dependent on road conditions and their performance is limited and requires a lot of training.

Combination Method. Considering the advantages and disadvantages of various methods, researchers usually combine two or more methods to driver's drowsiness. Lee et al. [20] detect driver alertness by wearable motion and physiological sensors and achieves an accuracy of over 96%. This work requires a PPG sensor connected to a wrist-wearable device to collect a PPG signal from the driver's finger. Then, through the low-power Bluetooth module, it transmits PPG data to the smartwatch in real time. dWatch directly collects heart rate data through a smartwatch to extract heart rate variability features without the need of a PPG sensor to collect finger PPG signals, and is more convenient and practical with faster data processing. Moreover, dWatch has higher accuracy in detecting not only heart rate variability and steering wheel movement characteristics, but also driver yawning behavior through heart rate data. Chang et al. [26] and Sun et al. [31] use the camera to capture the driver's facial image to obtain the characteristics of the yawning mouth. The image is then combined with the wireless ECG sensor to develop a smart driving assistance system. This method is based on the driver's facial image to detect yawning behavior, while dWatch performs detection using the heart rate change waveform. Hence, dWatch is more secure as it does not leak user privacy, and is more acceptable to users. Moreover, in these methods, the heart rate detection adopts an ECG sensor patch and the contact measurement is not as convenient as dWatch.

dWatch uses a convenient way for signal detection without using dedicated equipment. Although the measured physiological signals are not as accurate as those from professional equipment, the overall detection accuracy of the system is significantly improved by fusing the physiological and driving behavior characteristics of the driver. Moreover, dWatch is much less expensive than any dedicated equipment and can be implemented as an add-on to existing equipment. Compared with CV-based methods, dWatch uses driver physiological signals and behavioral features to detect driver fatigue without violating user privacy, and the combined signals ensure robustness under lights, obstructions, and the like. In some scenarios, the movement characteristics are not caused by the driver's operation, but the road changes. Compared with the method based on a motion sensor, dWatch detects physiological signals that can truly reflect the fatigue state of the driver and hence exhibits higher reliability. We would also like to point out that unlike smartphones, smartwatches oftentimes need to be charged offline, and hence power efficiency is particularly important in the design.

7 CONCLUSION

This article presents dWatch, a real-time driver drowsiness detection system that combines the physiological performance and motion state of the driver. dWatch extracts HRV features related to drowsiness from heart rate data using statistical methods and detects whether the driver yawns through a heart rate sequence yawn matching model (HYM). Then, the data collected by the motion sensor such as an accelerometer is used to track the movement of the driver's hand, which is further used to infer the movement of the steering wheel of the vehicle. The motion data not only assists in detection, but also acts as a starting mechanism for activating the heart rate sensor; hence reducing the power consumption of the system. dWatch employs an adaptive

training process that handles significant changes in the driver's movement characteristics during driving. The extracted physiological features and motion features are used as the parameters of a SVM method to obtain the driver's drowsiness state. Extensive experimental results show that dWatch achieves an accuracy of 97.1% and a recall of 98.3%, and saves 33% of energy.

REFERENCES

[1] Erika Abe, Koichi Fujiwara, Toshihiro Hiraoka, Toshitaka Yamakawa, and Manabu Kano. 2014. Development of drowsy driving accident prediction by heart rate variability analysis. In *Proceedings of the Asia-Pacific Signal and Information Processing Association Annual Summit and Conference (APSIPA 2014)*. IEEE, 1–4. DOI: https://doi.org/10.1109/APSIPA.2014.7041787

[2] Kofi Sarpong Adu-Manu, Nadir Adam, Cristiano Tapparello, Hoda Ayatollahi, and Wendi Heinzelman. 2018. Energy-harvesting wireless sensor networks (EH-WSNs): A review. *ACM Trans. Sen. Netw.* 6, 2, Article 10 (4 2018), 50 pages.

[3] Muhammad Awais, Nasreen Badruddin, and Micheal Drieberg. 2017. A hybrid approach to detect driver drowsiness utilizing physiological signals to improve system performance and wearability. *Sensors* 17 (08 2017), 1991. https://doi.org/10.3390/s17091991

[4] Anda Baharav, Suresh Kotagal, Vincent Gibbons, Bruce Rubin, G. Pratt, J. Karin, and S. Akselrod. 1995. Fluctuation in autonomic nervous activity during sleep displayed by power spectrum analysis of heart rate variability. *Neurology* 45, 6 (07 1995), 1183–1187. DOI: https://doi.org/10.1212/WNL.45.6.1183

[5] Chongguang Bi, Jun Huang, Guoliang Xing, Landu Jiang, Xue Liu, and Minghua Chen. 2017. SafeWatch: A wearable hand motion tracking system for improving driving safety. In *Proceedings of the 2nd International Conference on Internet-of-Things Design and Implementation (IoTDI'17)*. ACM, New York, 223–232. DOI: https://doi.org/10.1145/3054977.3054979

[6] Roman Bittner, Pavel Smrcka, Miroslav Pavelka, Petr Vysoky, and Lubomir Pousek. 2001. Fatigue indicators of drowsy drivers based on analysis of physiological signals. In *Proceedings of the 2nd International Symposium on Medical Data Analysis (ISMDA'01)*. Springer-Verlag, London, UK, 62–68. http://dl.acm.org/citation.cfm?id=646351.691016

[7] Dongyao Chen, Kyong-Tak Cho, Sihui Han, Zhizhuo Jin, and Kang G. Shin. 2015. Invisible sensing of vehicle steering with smartphones. In *Proceedings of the 13th Annual International Conference on Mobile Systems, Applications, and Services (MobiSys'15)*. ACM, New York, 1–13. DOI: https://doi.org/10.1145/2742647.2742659

[8] Timothy P. Corey, Elana B. Gordis Melanie L. Shoup-Knox, and Gordon G. Gallup Jr. 2012. Changes in physiology before, during, and after yawning. *Frontiers in Evolutionary Neuroscience* 3, 7 (2012). DOI: https://doi.org/10.3389/fnevo.2011.00007

[9] Taner Danisman, Ian Marius Bilasco, Chabane Djeraba, and Nacim Ihaddadene. 2010. Drowsy driver detection system using eye blink patterns. In *Proceedings of the 2010 International Conference on Machine and Web Intelligence*. IEEE, 230–233. DOI: https://doi.org/10.1109/ICMWI.2010.5648121

[10] Ioanna Chouvarda Emmanouil Michail, Athina Kokonozi and Nicos Maglaveras. 2008. EEG and HRV markers of sleepiness and loss of control during car driving. In *Proceedings of the IEEE 2008 30th Annual International Conference of Engineering in Medicine and Biology Society*. IEEE, 2566–2569. DOI: https://doi.org/10.1109/IEMBS.2008.4649724

[11] Ruijia Feng, Guangyuan Zhang, and Bo Cheng. 2009. An on-board system for detecting driver drowsiness based on multi-sensor data fusion using Dempster-Shafer theory. In *Proceedings of the 2009 International Conference on Networking, Sensing and Control*. 897–902. DOI: https://doi.org/10.1109/ICNSC.2009.4919399

[12] Gabriela Dorfman Furman, Armanda Baharav, and C. Cahanand Solange Akselrod. 2008. Early detection of falling asleep at the wheel: A heart rate variability approach. In *Proceedings of the 2008 Conference on Computers in Cardiology*. IEEE, 1109–1112. DOI: https://doi.org/10.1109/CIC.2008.4749240

[13] Vrushali B. Ghule and S. S. Katariya. 2015. Drowsiness detection methods for drivers: A review. *International Journal of Computer Applications* 122, 19 (7 2015), 36–38. https://doi.org/10.5120/21812-5141

[14] Adrian G. Guggisberg, Johannes Mathis, Armin Schnider, and Christian W. Hess. 2011. Why do we yawn? The importance of evidence for specific yawn-induced effects. *Neuroence and Biobehavioral Reviews* 35, 5 (2011), 1302–1304. DOI: https://doi.org/10.1016/j.neubiorev.2010.12.004

[15] Sinh Huynh, Rajesh Krishna Balan, JeongGil Ko, and Youngki Lee. 2019. VitaMon: Measuring heart rate variability using smartphone front camera. 1–14. In *Proceedings of the 17th Conference on Embedded Networked Sensor Systems (SenSys'19)*. ACM, New York, DOI: https://doi.org/10.1145/3356250.3360036

[16] Masrullizam Mat Ibrahim, John J. Soraghan, Lykourgos Petropoulakis, and Gaetano Di Caterina. 2015. Yawn analysis with mouth occlusion detection. *Biomedical Signal Processing and Control* 18 (2015), 360–369. DOI: https://doi.org/10.1016/j.bspc.2015.02.006

[17] Mahdi Ilbeygi and Hamed Shah-Hosseini. 2012. A novel fuzzy facial expression recognition system based on facial feature extraction from color face images. *Eng. Appl. Artif. Intell.* 25, 1 (2 2012), 130–146. DOI: https://doi.org/10.1016/j.engappai.2011.07.004

[18] Samuel Lawoyin, Ding-Yu Fei, and Ou Bai. 2015. Accelerometer-based steering-wheel movement monitoring for drowsy-driving detection. In *Proceedings of the Institution of Mechanical Engineers, Part D: Journal of Automobile Engineering* 229, 2 (2015), 163–173. http://dx.doi.org/10.1177/0954407014536148

[19] Samuel Lawoyin, Xin Liu, Ding-Yu Fei, and Ou Bai. 2014. Detection methods for a low-cost accelerometer-based approach for driver drowsiness detection. In *Proceedings of the 2014 IEEE International Conference on Systems, Man, and Cybernetics (SMC)*. IEEE, 1636–1641. DOI: https://doi.org/10.1109/SMC.2014.6974150

[20] Boon-Giin Lee, Boon-Leng Lee, and Wan-Young Chung. 2015. Smartwatch-based driver alertness monitoring with wearable motion and physiological sensor. In *Proceedings of the 2015 37th Annual International Conference of the IEEE Engineering in Medicine and Biology Society (EMBC)*. IEEE, 6126–6129. DOI: https://doi.org/10.1109/EMBC.2015.7319790

[21] Gang Li and Wan-Young Chung. 2013. Detection of driver drowsiness using wavelet analysis of heart rate variability and a support vector machine classifier. *Sensors* 13, 12 (2013), 16494–16511. DOI: https://dx.doi.org/10.3390%2Fs131216494

[22] Gang Li, Boon Leng Lee, and Wan-Young Chung. 2015. Smartwatch-based wearable EEG system for driver drowsiness detection. *IEEE Sensors Journal* 15, 12 (12 2015), 7169–7180. DOI: https://doi.org/10.1109/JSEN.2015.2473679

[23] Zuojin Li, Shengbo Li, Renjie Li, Bo Cheng, and Jinliang Shi. [n.d.]. Online detection of driver fatigue using steering wheel angles for real driving conditions. *Sensors* 17, 3 ([n.d.]), 495. DOI: https://doi.org/10.3390/s17030495

[24] Zhenjiang Li, Yunhao Liu, Mo Li, Jiliang Wang, and Zhichao Cao. 2013. Exploiting ubiquitous data collection for mobile users in wireless sensor networks. *IEEE Transactions on Parallel and Distributed Systems* 24, 2 (2 2013), 312–326. DOI: https://doi.org/10.1109/TPDS.2012.92

[25] Yufeng Lu and Zengcai Wang. 2007. Detecting driver yawning in successive images. In *Proceedings of the 2007 1st International Conference on Bioinformatics and Biomedical Engineering*. IEEE, 581–583. DOI: https://doi.org/10.1109/ICBBE.2007.152

[26] Yu lung Chang, Yen cheng Feng, and Oscal T. C. Chen. 2016. Real-time physiological and facial monitoring for safe driving. In *Proceedings of the 2016 38th Annual International Conference of the IEEE Engineering in Medicine and Biology Society (EMBC)*. 4849–4852. DOI: https://doi.org/10.1109/EMBC.2016.7591813

[27] Mehrdad Sabet, Reza Aghaeizadeh Zoroofi, Khosro Sadeghniiat Haghighi, and Maryam Sabbaghian. 2012. A new system for driver drowsiness and distraction detection. In *Proceedings of the 20th Iranian Conference on Electrical Engineering (ICEE'12)*. IEEE, 1247–1251. DOI: https://doi.org/10.1109/IranianCEE.2012.6292547

[28] Ahmad Shahin Nermine Munla, Mohamad Khalil, and Azzam Mourad. 2015. Driver stress level detection using HRV analysis. In *Proceedings of the 2015 International Conference on Advances in Biomedical Engineering (ICABME)*. 61–64. DOI: https://doi.org/10.1109/ICABME.2015.7323251

[29] Rau Paul Stephen. 2005. Drowsy driver detection and warning system for commercial vehicle drivers. In *Field Operational Test Design, Data Analyses and Progress, National Highway Traffic Safety Administration of USA (NHTSA)*. 5–192.

[30] Arun Sahayadhas, Kenneth Sundaraj, and Murugappan Murugappan. 2012. Detecting driver drowsiness based on sensors: A review. *Sensors* 12, 12 (12 2012), 16937–16953. DOI: https://doi.org/10.3390/s121216937

[31] Chao Sun, Jian Li, Yang Song, and Lai Jin. 2013. Real-time driver fatigue detection based on eye state recognition. *Applied Mechanics and Materials* 457-458 (10 2013), 944–952. DOI: https://doi.org/10.4028/www.scientific.net/AMM.457-458.944

[32] Jose Vicente, Pablo Laguna, Ariadna Bartra, and Raquel Bailon. 2011. Detection of driver's drowsiness by means of HRV analysis. In *Proceedings of the 2011 Conference on Computing in Cardiology*. IEEE, 89–92.

[33] Zheng Yang, Lirong Jian, Chenshu Wu, and Yunhao Liu. 2013. Beyond triangle inequality: Sifting noisy and outlier distance measurements for localization. *ACM Trans. Sen. Netw.* 9, 2, Article 26 (4 2013), 20 pages. DOI: https://doi.org/10.1145/2422966.2422983

Received December 2019; revised May 2020; accepted June 2020